Design and Application of Wireless Tool Temperature Measurement of Friction Stir Welding (FSW) for Process Monitoring and Control

Jinsu Gim[1], Mingoo Cho[1], Jaehwang Kim[2], Kwang-Jin Lee[3],
Deva P. Neelakandan[4], Chanho Lee[4], Yoon Chul Jung[5] and Sungwook Kang[6*]

[1] Extreme Process Control Group, Korea Institute of Industrial Technology (KITECH), Jinju, 52845, Korea
[2] Carbon & Light Materials Group, Korea Institute of Industrial Technology (KITECH), Jeonju, 54853, Korea
[3] KITECH USA Technology Cooperation Center, San Jose, CA 95134, USA
[4] Department of Mechanical Engineering, Auburn University, Auburn, AL 36849, USA
[5] DnM Aerospace, Sacheon, 52535, Korea
[6] Department of Smart Ocean Mobility Engineering, Changwon National University, Changwon, 51140, Korea

* Corresponding author: Sungwook Kang, email: swkang@changwon.ac.kr

Abstract

This paper proposes a wireless friction stir welding (FSW) tool temperature measurement method, FSW process window, and control strategy based on the FSW tool temperature profiles. Tool temperature is important data for FSW process monitoring, optimization, and control because it includes detailed information on the actual FSW process condition where frictional heat is generated, and the workpiece material is softened and stirred. Conventionally, temperature data in the FSW process have been measured from thermocouples installed at workpieces or thermal imaging, which are indirect measurements. This study aims to develop a practical wireless FSW tool temperature measurement method and propose effective applications of the FSW tool temperature measurement for process monitoring, optimization, and control. The proposed wireless FSW tool temperature measurement system consists of a thermocouple-integrated FSW tool, data measurement, wireless data transmission modules based on widely used Internet of Things (IoT) devices, and a conventional tool holder. The developed system is capable to measure multiple temperature channels reliably at a high sampling rate in real-time on the shop floor. Based on the tool temperature profiles measured under various FSW process conditions, tool temperature profile features indicating welding quality, and process window for stable welding quality are proposed. FSW process control strategy and process setup for the early FSW process stage based on the tool temperature measurement are also proposed. The proposed approach can not only improve FSW process monitoring and control but also contribute to data-based autonomous manufacturing as well as relieve the tacit knowledge aspect of the FSW process.

Graphical Abstract

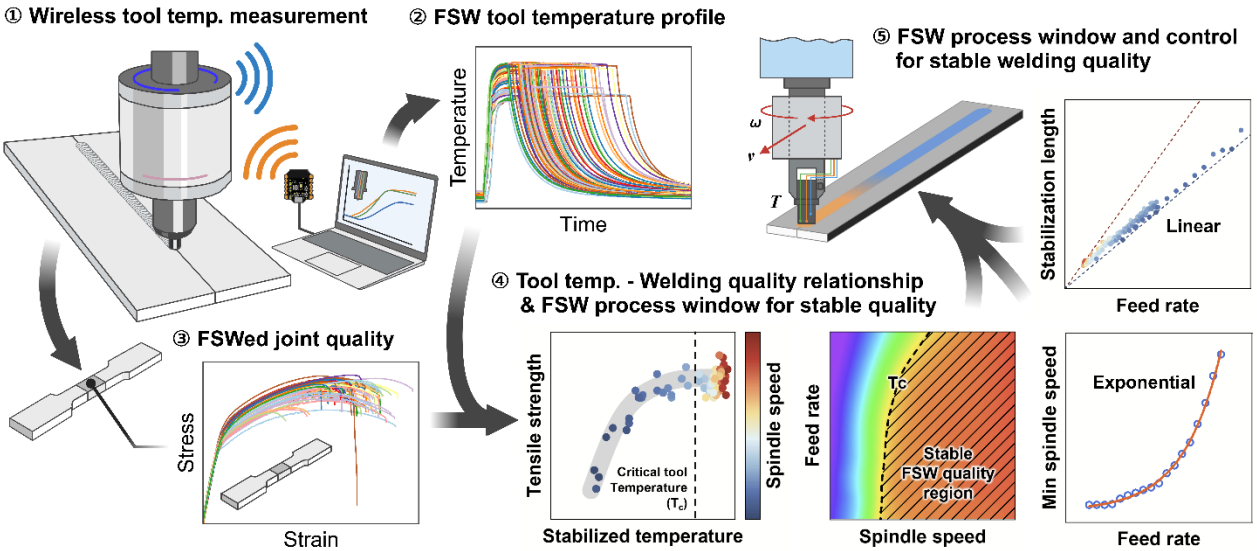

Keywords

Friction stir welding, wireless monitoring, tool temperature, welding quality, FSW monitoring, FSW control

Highlights

- The proposed approach can measure FSW tool temperature wirelessly in real-time.
- The relationship between FSW tool temperature profiles and welding quality is analyzed.
- A temperature feature indicating welding quality, and a process window for stable quality are proposed.
- FSW process control strategies based on tool temperature measurement are proposed.
- This approach improves FSW process monitoring and control, and contributes to data-based manufacturing.

1. Introduction

Friction stir welding (FSW) is welding technology without melting the workpiece material by stirring softened material using frictional heat generation from the rotation of non-consumable tools and pressure [1–3]. FSW, which was first proposed by TWI (The Welding Institute, UK) has several advantages such as minimized cracks and defects due to the non-melting process [4–7], small thermal deformation due to lower processing temperature than melting temperature [8], and good mechanical strength of the welding joint [9,10]. Furthermore, FSW is an efficient and minimized environmental and health effect process because it does not require additional fillers, protective gases [11,12], or consumable tools, and harmful rays and gases are not generated in the process, respectively [13,14]. These advantage of FSW make it applicable to welding of various materials such as dissimilar and nonferrous metals [15,16], polymer and plastics [17], and composites for aerospace, railway, and shipbuilding industries [18,19].

Quality of FSWed joints is influenced by heat generation during the welding process [20–25]. The frictional heat generation is influenced by various factors such as tool rotation speed [26,27], feed rate [28,29], downward force or pressure, tool geometry including diameter and pattern of shoulder and probe [30–33]. Among these factors, tool rotation speed, feed rate, plunge depth, and axial force are controlled by closed-loop control to optimized FSWed joint quality [34,35]. However, conventional FSW control methods are difficult to consider the real-time temperature variation during the process.

Optimization of FSW process parameters and prediction of FSWed joint quality have been investigated. Several researchers emphasized that prediction of maximum temperature during the FSW process is important to ensure FSWed joint quality, and minimize welding defects. Anadan et al. predicted the maximum temperature using machine learning (ML) based on thermal images and temperature measured by thermocouple installed into the workpieces [36]. Sarvaiya et al. developed artificial neural network (ANN) to predict the maximum temperature and micro hardness [37]. Most of the studies focusing on the temperature in the FSW process have measured temperature of workpiece, not the FSW tool. Measuring workpiece temperature is difficult to apply in situ FSW process control in consideration of temperature variation flowing the FSW tool movement because thermal accumulation in the FSW tool cannot be considered and installing multiple temperature sensors along the whole welding line is impossible for practical applications.

Several methods to measure the temperature at the FSW tool have been proposed. The tool-workpiece-thermocouple (TWT) method proposed by De Backer et al. measured interface temperature at the FSW tool and workpiece using the thermoelectric effect from material difference in the FSW tool and workpiece [38]. This method required calibration of a thermoelectric voltage-temperature relationship between a specific combination of the FSW tool and workpiece materials. A wireless FSW tool temperature measurement method has been proposed by Schmale et al. using thermocouple insertion at the tool-workpiece interface and Bluetooth-based wireless DAQ (data acquisition) system, and used for tool temperature-based closed-loop control [39]. Similarly, Fsilva et al. proposed the FSW tool temperature measurement using the thermocouple-inserted FSW tool and slip ring [40]. These methods had limitations due to the required calibration for different tool and workpiece materials, exposed thermocouples at the tool-workpiece interface under high mechanical stress during the process, and contact-based measurement susceptible to wear and noise.

This paper proposes a wireless FSW tool temperature measurement method based on the thermocouple-integrated FSW tool and real-time wireless data transmission for FSW process monitoring and control, as described in the schematic, Fig. 1. Transient tool temperature profiles are measured under various FSW process conditions, and relationships among the FSW process parameters, tool temperature profiles, and FSWed joint quality were analyzed. Based on the proposed FSW tool temperature measurement, FSW process window and process setup for stable welding quality, and control strategy are proposed. At the end of this paper, the industrial implications, limitations, and future scope of this research will be discussed.

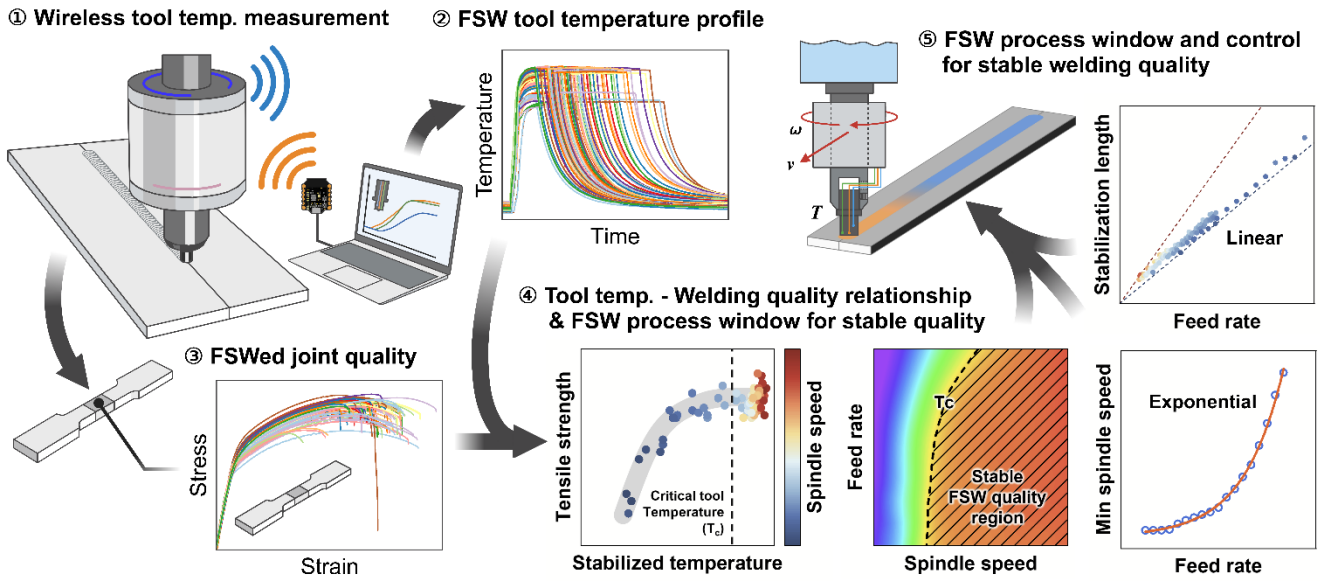

Fig. 1 Schematic of the overall workflow of this research for FSW process window and control for stable welding quality based on the wireless FSW tool temperature measurement.

2. Methodology

2.1. Wireless FSW tool temperature measurement

A wireless temperature measurement system is required for the FSW tool temperature measurement because the tool rotates fast during the FSW process. Therefore, a wireless measurement system was devised using IoT (Internet of Things) devices which are easily supplied conventionally. The developed FSW tool temperature measurement system consists of (1) a thermocouple-integrated FSW tool, (2) a data acquisition and wireless data transmitter (TX), and (3) a wireless data receiver (RX) and control PC.

2.1.1. Thermocouple-integrated FSW tool

Multiple temperature measurement positions were determined in the FSW tool to consider temperature distribution inside. Frictional heat for softening the material is generated at the interface between the workpiece and both the probe and shoulder. The generated heat is transferred from the center to the outer perimeter of the tool (radial direction) and from the tool to the tool holder (axial direction). Therefore, the temperature gradient was assumed to be distributed along the radial and axial directions simultaneously. To consider the temperature gradient, three thermocouples were flush-mounted at different radii and depths in the tool as shown in Fig. 2a. It was difficult to guarantee precise machining of the thermocouple hole depths due to the high aspect ratio. Therefore, the depth of thermocouple junctions was set by thermocouple length not the depth of thermocouple holes after machining of the thermocouple holes above 1 mm from the shoulder surface. Fig. 2b represents the FSW tool after machining. The tool was fabricated by hot work tool steel, SKD61 and it was considered as sufficient because the workpiece material was aluminum.

Electrically insulative and highly heat conductive adhesive was used to fix thermocouples into the tool for improved stability and sensitivity of the tool temperature measurement. Conventional sheath-type thermocouple has a thermocouple junction inside of the metal sheath, and the insulation material such as ceramic fills the inside volume. Metal sheath and insulation make the sheath-type thermocouples very rigid and robust against mechanical stress and external electric noise. However, sensitivity is lower than bare junction type thermocouples due to the long heat transfer path from the sheath to thermocouple junction and heat transfer through insulation filling. It was assumed that the heat transfer path consisting of the tool-thermocouple cement (heat transfer medium)–sheath-insulation-thermocouple junction is too long, and the temperature profile would be insensitive to

tool temperature variation. Therefore, bare junction-type thermocouples were installed into the tool. The medium between the tool and thermocouple junctions should be highly heat conductive and electrically insulative for sensitive temperature measurement and insensitive to external electric noise from the FSW machine. Furthermore, the medium should be stable in high temperatures up to 500 ˚C developed in the FSW process. The used heat transfer medium was oxidized aluminum (Al_2O_3)-based and electrically insulative adhesive with 5.77 W/(m·K) of thermal conductivity, and maximum 1,800 ˚C of operation temperature (Resbond 903HP, Cotronics Corp., USA).

Figs. 2c–e present the thermocouple installation procedure. As shown in Fig. 2c, thermocouple junctions were welded and then coated by the adhesive. The adhesive was cured at 315 ˚C temperature condition in a furnace. The coated thermocouple was inserted into the holes previously filled by injected adhesive as shown in Fig. 2d. The remaining adhesive was cured in the same condition. As a cross-sectional image of the FSW tool, Fig. 2f, the position of the thermocouple junctions was verified by X-ray μCT (XTH-450, Nikon Metrology NV, UK).

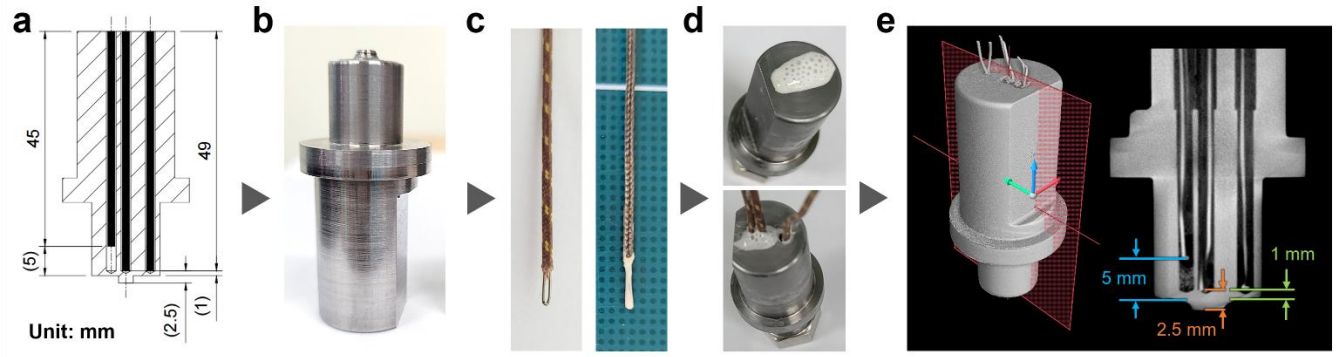

Fig. 2 Design and fabrication of a thermocouple-integrated friction stir welding (FSW) tool. **a** Design of the FSW tool with thermocouple holes. **b** The machined FSW tool. **c** Coating of thermocouple junction bead and bare wires using highly heat conductive and electrically insulative adhesive. **d** Pre-injection of the adhesive into the thermocouple holes and insertion of thermocouples. **e** Validation of thermocouple positions using μCT image.

2.1.2. Wireless temperature measurement system

It was required to devise a wireless temperature measurement system to measure the rotating FSW tool temperature because conventional wired measurement methods are not suitable. Conventional contact-based electric circuits such as slip ring are unacceptable for long-term industrial applications due to friction-induced wear. Especially for temperature measurement, the weak thermoelectric voltage from thermocouples is susceptible to electric noise caused by unstable electric connections. Thanks to the recently developed various IoT devices, such DAQ system with wireless data transmission can be easily devised at low cost.

The developed wireless FSW tool temperature measurement system was constructed as shown in Fig. 3a. The central device measuring analog signals and transmitting wireless data was Arduino-based single board computer (SBC), Beetle BLE (DFRobot Corp., China). It was appropriate to devise a low-power wireless communication system because it supports Bluetooth low energy (BLE). Thermocouple amplifiers (AD8495, Analog Devices, Inc., USA) for thermocouple, and conventional battery cells (AAA × 4) for easily replaceable power supply were connected as well.

A measurement base was designed to support the components steady in high rotation speed and fix them to a conventional tool holder (BT50-SLA20-250, Sekwang Selux Co., Ltd, Korea). Each component was allocated on each side of the base with consideration of balance, and 3D-printed ABS covers were attached to the base, as shown in Fig. 3b. The thermocouples were connected to thermocouple amplifiers through one of the set screw holes and slot in the base. Fig. 3c presents an example of the actual usage of the system. The system had no mechanical or electrical issues up to 3,000 rpm of spindle rotation speed and 100 cycles of consecutive FSW process. The FSW process setup using the wireless tool temperature measurement is shown in Fig. 3d.

The rotating wireless FSW tool temperature measurement system was a data transmitter (TX) of the temperature data, and another SBC and PC were a data receiver (RX) as shown in Fig. 3e. The TX and RX modules transmitted data through BLE serial communication. The single measurement cycle was started by measuring time input from a user to a PC running a Python-based program. During the measurement, profiles of all temperature channels were plotted in real-time. After the end of measurement time, final temperature profiles were plotted and saved, as presented in Fig. 3f. Up to 1 kHz sampling speed was possible for three temperature measurement channels, but the temperature data were measured by 100 Hz of sampling speed for long battery life.

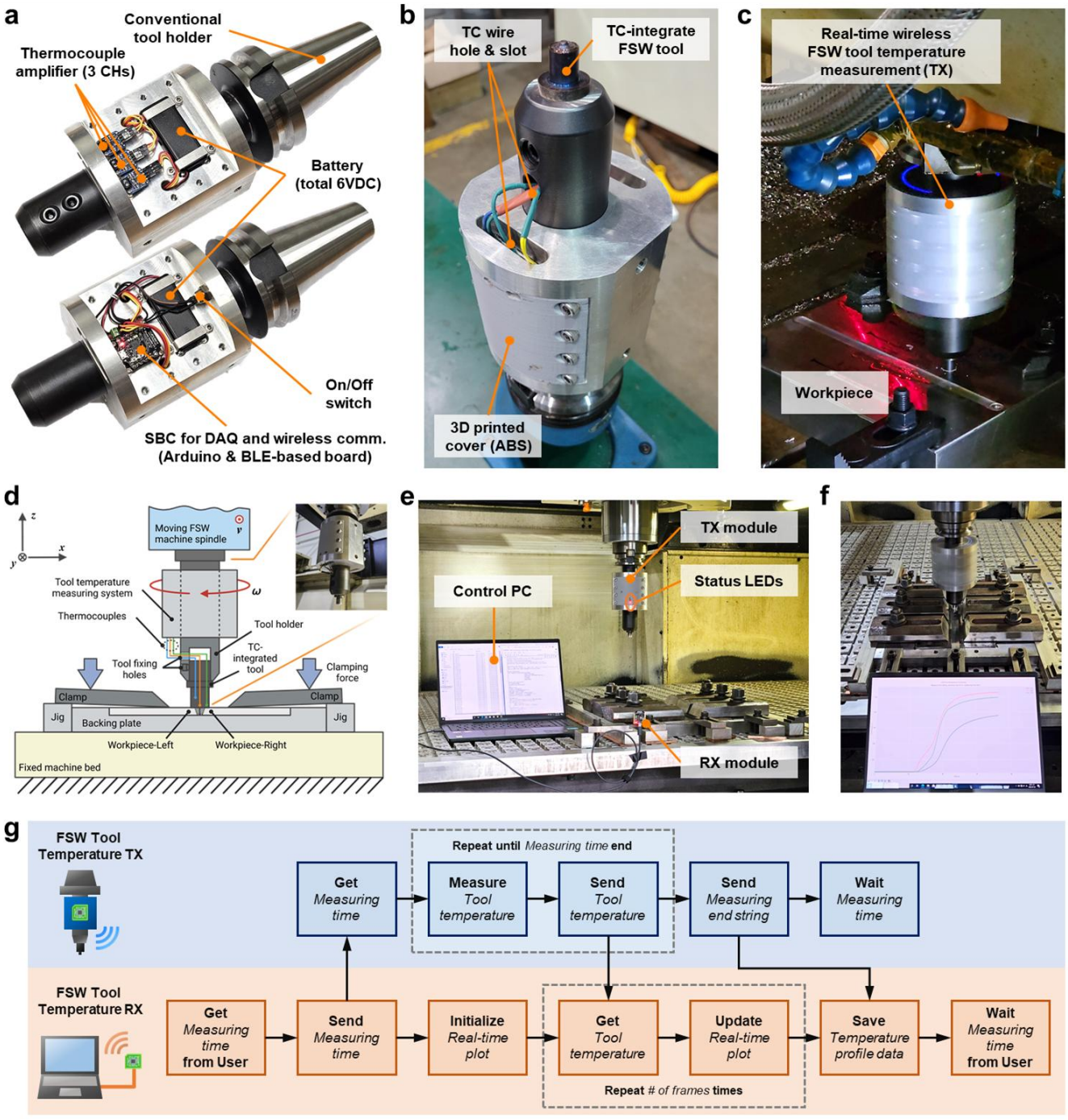

Fig. 3 Real-time wireless FSW tool temperature measurement system. **a** Main component consisting of the measurement system. **b** Assembled measurement system with a tool holder, the thermocouple (TC)-integrated FSW tool, and covers. **c** Application of the measurement system in the FSW process. **d** Schematic of the FSW process setup with the wireless FSW tool temperature measurement. **e** Transmitter (TX) and receiver (RX) modules of the measurement system. **f** Real-time plot of the FSW tool temperature profiles. **g** Flow chart of the program imbedded in the TX module and implemented in the RX module and PC.

2.2. Design of experiment (DoE)

2.2.1. FSW process range

Experimental conditions were determined to minimize overlapping process parameter values to measure the tool temperature in as various as possible FSW process conditions. Spindle rotation speed and feed rate were selected as process variables in this study because they are representative parameters of the FSW process. As a result of the preliminary test, the maximum feed rate was 500 mm/min to guarantee sufficient formation of tool temperature stabilized region in a 300 mm length aluminum workpiece for extraction of mechanical test specimens as shown in Fig. 4a. The feed rate range 500–1,000 mm/min was ambiguous for formation of tool temperature stabilized region. Therefore, the main FSW process range was set as 500–2500 rpm of spindle rotation speed, and 100–500 mm/min of feed rate. The extended process range was set as 500–1000 mm/min of feed rate. Hammersley Sequence Sampling (HSS) was applied to determine not overlapping and even distribution of experimental condition sampling in the process range. A total of 90 conditions and 10 conditions were determined in the main and extended process range, respectively, as shown in Fig. 4b. The used aluminum plates as workpieces were Al6061-T6 with 100×300×2 (width × length × thickness) mm. A conventional machining center (Hartford HEP-3150, She Hong Industrial Co., Ltd., Taiwan) was used as FSW machine for this study.

2.2.2. Welding quality test

Tensile specimens were extracted from the tool temperature stabilized region to analyze the correlation between measured tool temperature profiles and welding quality. The position of extracted tensile specimens is presented in Fig. 4a. The geometry of the specimen flowed ASTM E8-13a subsize type specimen geometry. The specimens were extracted by wire electro-discharge machining (EDM). The extracted specimens are shown in Fig. 4c.

Ultimate tensile strength (UTS) was determined as welding quality of FSWed joint. A tensile test machine (Criterion Model 45, MTS Systems Corp., USA) with an extensometer was used for tensile tests as shown in Figs. 4d and e. Fig. 4f presents the fractured specimens. All strain-stress curves are presented in Fig. 4g and UTS distribution is shown in Fig. 4h. The overall UTS was mainly distributed in 200–240 MPa, which is about 65–80% UTS range of the original workpiece material. It was considered as normal UTS reduction in not heat treated FSWed joint because strength enhancing factors were eliminated by the heat generation in the FSW process.

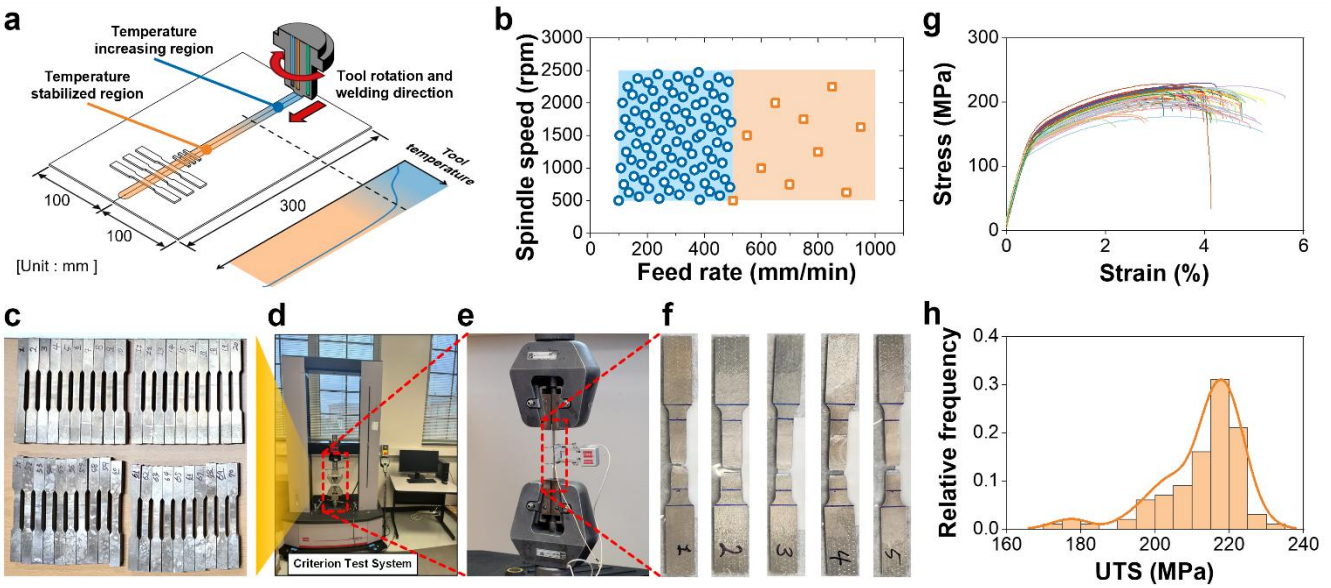

Fig. 4 Mechanical test specimen preparation. **a** Position of tensile specimens and geometry of the FSWed aluminum workpiece. **b** Sampling of FSW conditions using Hammersley Sequence Sampling (HSS). **c** Extracted tensile specimens. **d, e** The used tensile testing machine and tensile test setup. **f** Examples of the fractured tensile specimens. **g** Strain-stress curves of all the tested specimens. **h** Distribution of the ultimate tensile strength (UTS) of the tested specimens.

3. Results

3.1. Transient FSW tool temperature

Temperature profiles measured from the FSW tool present actual welding conditions in detail, therefore it contains various information on the process. This is because the tool temperature is closer to the actual FSW process condition where the frictional heat is generated and softened material is stirred than the preliminary set process parameters to the FSW machine.

The stages of the FSW process shown in Fig. 5a correlated with the transient FSW tool temperature profiles as presented in Fig. 5b. The tool temperature was similar to the ambient temperature in the “tool downward movement” stage before tool-workpiece contact. In the “tool plunging” stage with frictional heat generation, the temperature measured at the probe position was increased at first among the different thermocouple positions. Right after that, the temperature at the shoulder positions was increased due to the heat transfer from the probe. In the “shoulder touch and dwell” stage, additional heat generation between the shoulder and workpiece increased the temperature at a clearly higher rate than in the prior stage. The temperature measured at deep shoulder position (shoulder, distance 5 mm) showed lagged response approximately 0.5 s later than the other positions closer to the probe and shoulder surface, as shown in Fig. 5c. In the “tool forward” stage, the tool temperatures were stabilized according to the balance of heat generation and loss related to frictional heat generation, heat loss from the tool to both tool holder and spindle, heat loss by thermal radiation, flowing in of cold workpiece material, and flowing out of hot workpiece material.

Tool temperature profiles represented the actual effect of the FSW process parameters in welding conditions. Figs. 5d–f present various tool temperature profiles according to the combination of high/low spindle rotation speed and feed rate. In the case of the low spindle rotation speed conditions shown in Figs. 5d and f, the stabilized tool temperature at each position was lower than the high spindle rotation speed conditions shown in Figs. 5e and g because the frictional heat generation is smaller. In the case of the high feed rate conditions shown in Figs. 5f and g, the FSW process finished in a shorter processing time than low feed rate conditions shown in Figs. 5d and e because of the limited length of the welding line.

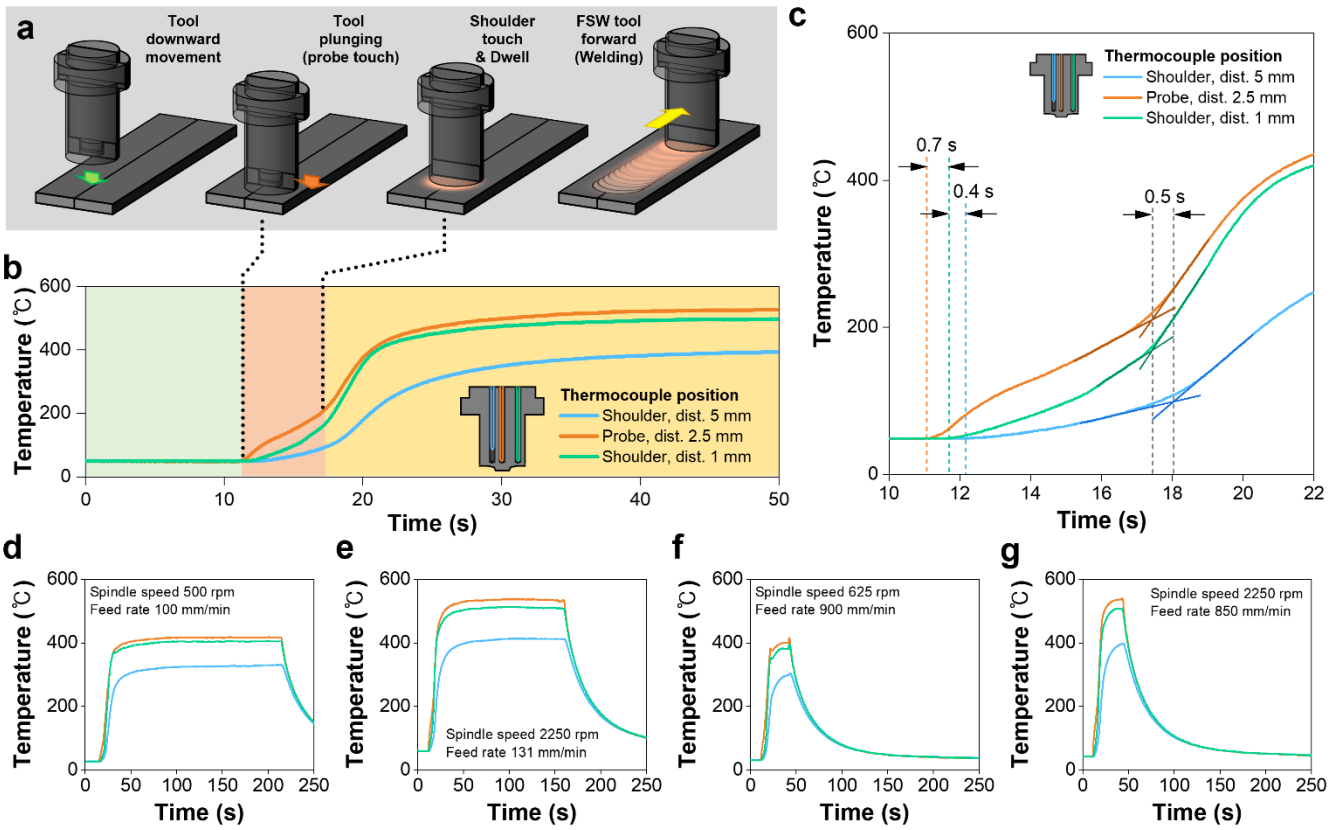

Fig. 5 Correlation of the FSW process stages and various tool temperature profiles. **a** FSW process stages. **b** FSW tool temperature profiles measured at difference positions and depths. **c** Enlarged temperature profiles and time lag between the profiles. Examples of FSW tool temperature profiles at **d** low – low, **e** high – low, **f** low – high, and **g** high – high spindle rotation speed and feed rate in predetermined DoE range, respectively. Note: The meaning line colors in **d**–**g** is the same to **b** and **c**.

3.2. Influence of FSW process parameters on tool temperature

Representative features in each temperature profile should be extracted for comparison, because the tool temperature profiles are time-series data and direct comparison is difficult. Three feature points shown in Fig. 6a were defined by referring to the temperature increase and then the stabilizing trend. The stabilized tool temperature, $\boldsymbol{T_{stbl}}$ was extracted by averaging 2.00 s data in temperature stabilized region. The sudden increase of the temperature at the end of the process as shown in Fig. 5f was neglected by excluding the final 4.0 s temperature data. The characteristic time, $\boldsymbol{t_1}$, and $\boldsymbol{t_2}$ were determined as features representing temperature stabilization speed in the early FSW stages. These features were determined by referring to the widely used thermal time constant. The features were defined by the required time to reach 63.2% ($\boldsymbol{1-e^{-1}}$) and 86.5% ($\boldsymbol{1-e^{-2}}$) of $\boldsymbol{\Delta T}$ from the onset of the temperature increase. $\boldsymbol{\Delta T}$ was the temperature difference between the initial temperature and $\boldsymbol{T_{stbl}}$. Among the temperature profiles, the probe temperature profile was selected to extract temperature profile features due to the earliest onset of temperature increase and the highest $\boldsymbol{T_{stbl}}$.

The extracted features represented the detailed effect of the FSW process parameters on tool temperature conditions. Figs. 6b and c are the variations of stabilized tool temperature according to the FSW process parameters. The stabilized tool temperature was distributed widely according to the feed rate shown in Fig. 6b. The minimum stabilized tool temperature seemed to decrease at a higher feed rate. Therefore, it was supposed that the feed rate decreases the stabilized tool temperature. The main cause could be a faster flow-in rate of the cold workpiece material and flow-out rate of the hot workpiece material under the FSW tool by higher feed rate conditions. In comparison with the feed rate, spindle rotation speed directly affected the stabilized tool

temperature as shown in Fig. 6c. Interestingly, this trend was especially strong in the low spindle rotation speed range <1,100 rpm as 20 ˚C/100 rpm ratio up to approximately T_{stbl}=510 ˚C. In the high spindle rotation speed range >1,100 rpm, the stabilization temperature increasing rate was dropped to 1.5 ˚C/100 rpm. It seemed that 1,100 rpm is the critical spindle rotation speed or 510 ˚C is the critical tool temperature for the tested FSW process. The effect of the feed rate was considerable for t_1, and t_2 presenting temperature stabilization speed as shown in Figs. 6d and f in contrast to the insignificant effect of the spindle rotation speed as shown in Figs. 6e and g. It means that regardless of the spindle rotation speed, the tool temperature is stabilized earlier in the higher feed rate conditions.

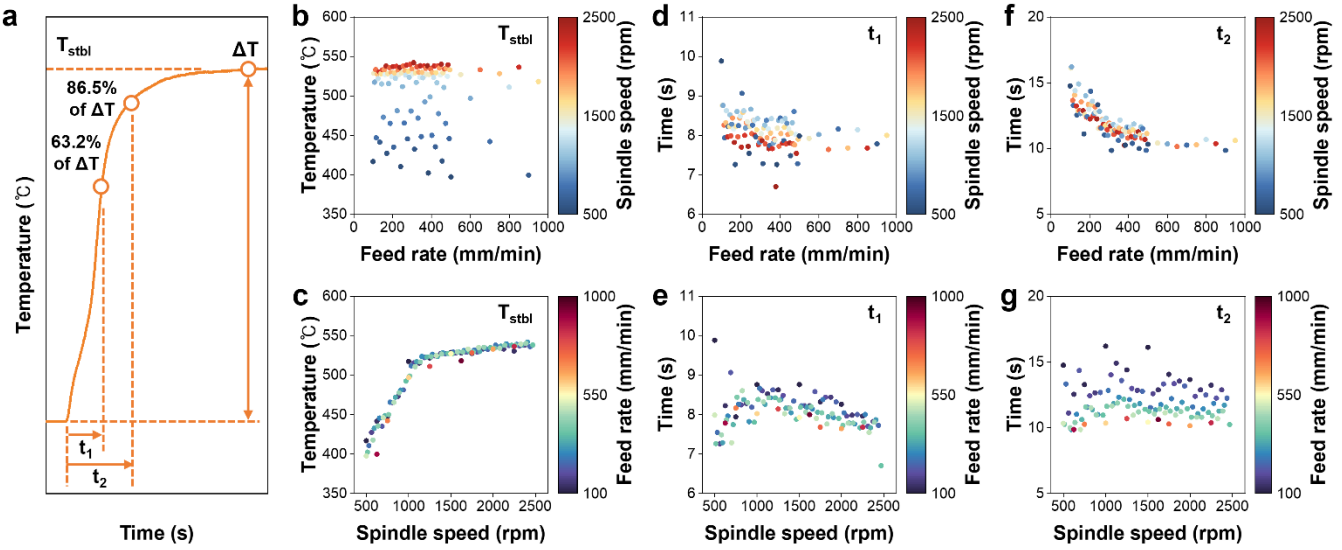

Fig. 6 Correlations between FSW tool temperature profile features and FSW process parameters. **a** Definition of transient tool temperature profile features. **b**, **c** Stabilized tool temperature (T_{stbl}), **d**, **e** first characteristic time (t_1), **f**, and **g** second characteristic time (t_2) according to feed rate and spindle rotation speed, respectively.

3.3. Effect of tool temperature on welding quality

It was assumed that the temperature profile features would have solid relationships to welding quality because the features present characteristics of each FSW condition. Figs. 7a–d present the effect of the temperature profile features on UTS as welding quality. As shown in Figs. 7a and b, the UTS showed stabilizing trends depending on the stabilized tool temperature. The welding quality was converged to approximately 220 MPa of UTS in the range of T_{stbl}>510 ˚C. Therefore, 510 ˚C of the stabilized tool temperature can be regarded as the critical tool temperature (T_c) to achieve stable welding quality. This result is similar to the critical tool-workpiece interface temperature reported by Fehrenbacher et al. [41]. The main control parameter for this trend was the spindle rotation speed as shown in Fig. 7b (c.f., color bar) and Fig. 6c. The characteristic time, t_1, and t_2 showed insignificant effect on the welding quality as shown in Figs 7c and d. It can be regarded that temperature history in the early FSW process stages is insignificant to the welding quality in the welding line with stabilized tool temperature.

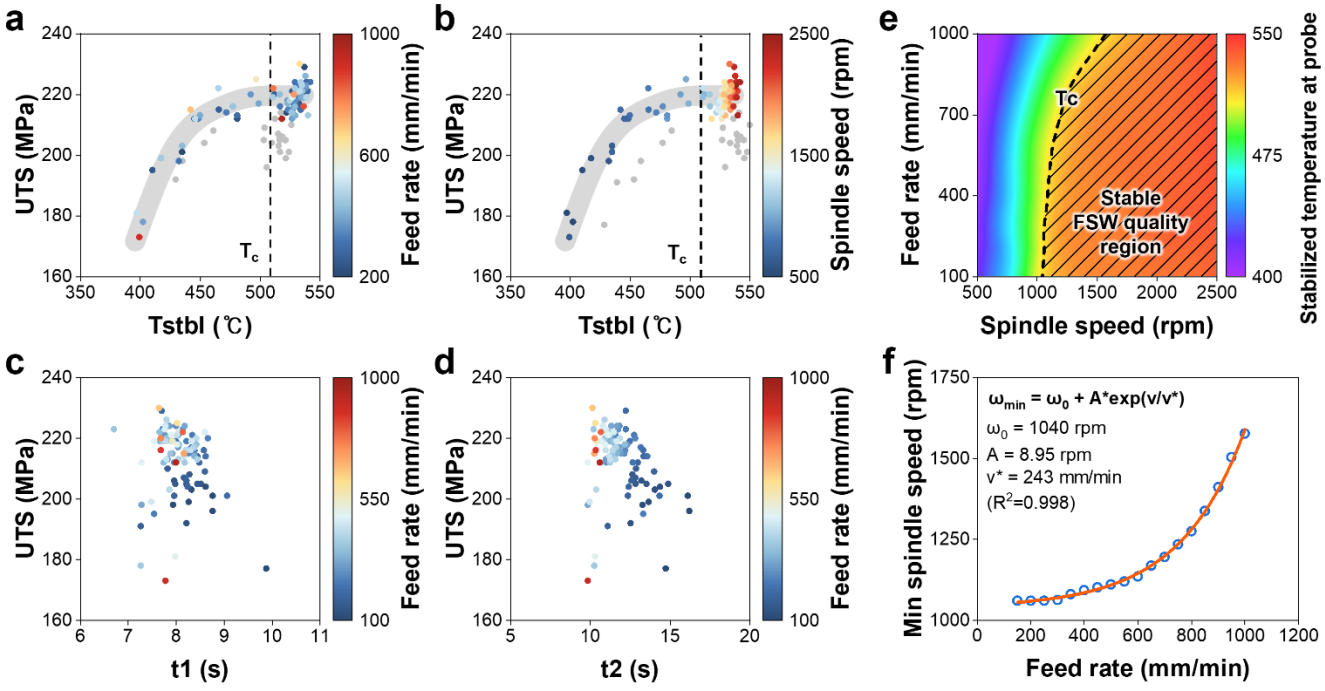

Fig. 7 Welding quality according to FSW tool temperature profile features, and control. UTS according to **a**, **b** stabilized temperature (T_{stbl}), **c**, **d** characteristic times (t_1, t_2). **e** FSW process window for stable UTS. **f** Required minimum spindle rotation speed (ω_{min}) in various feed rate (v) conditions. Note: The data points in the range of feed rate <200 mm/min are shown in gray color for better legibility of the relationship in **a** and **b**.

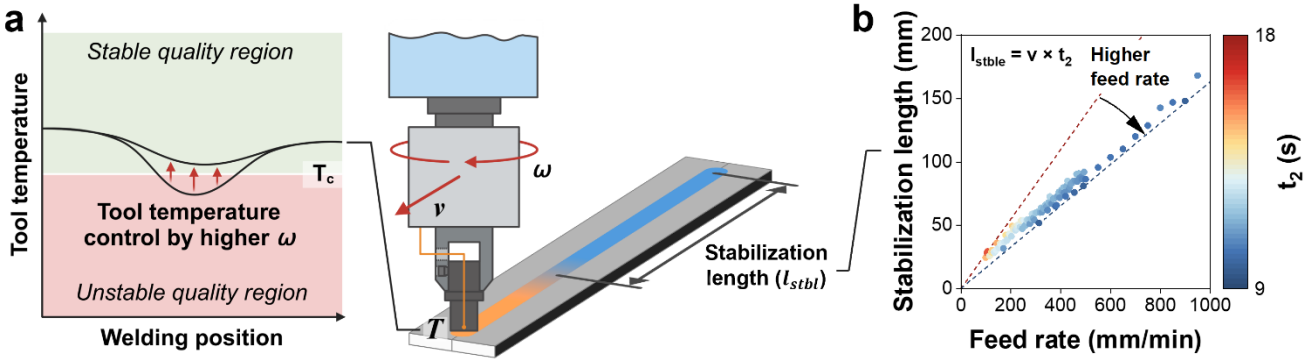

Fig. 8 Control of FSW process using wireless tool temperature measurement. **a** Tool temperature (T) control by spindle rotation speed (ω) based on the critical temperature (T_c). **b** Stabilization length (l_{stbl}) in various feed rate (v) conditions.

3.4. FSW process control for stable welding quality

3.4.1. FSW process window

The FSW process window for stable welding quality can be mapped based on the experimental data distributed well by the HSS DoE method, and the critical tool temperature as shown in Fig. 7e. It represents the variation of the stabilized tool temperature according to the FSW process parameters shown in Figs. 6b and c, and the stable welding quality window determined by the critical tool temperature, T_c. In the low feed rate <400 mm/min of FSW conditions, the required minimum spindle rotation speed was about 1,100 rpm. In the high feed rate >400 mm/min conditions, the required minimum spindle rotation speed increases gradually. This infers that higher spindle rotation speed is required to guarantee stable and better welding quality in the higher feed rate FSW process.

Fig. 7f presents this relationship between the required minimum spindle rotation speed (ω_{min}) to achieve the critical tool temperature in various feed rate conditions. Interestingly, the $\omega_{\min}$ showed an exponential relationship to the feed rate. It means that a much higher spindle rotation speed is required in higher feed rate conditions, and the FSW process window for stable welding quality might be limited by the maximum spindle rotation speed of the FSW machine, not the maximum feed rate. Maintaining the tool temperature above the critical tool temperature can be controlled by adjusting the spindle rotation speed as presented in Fig. 8a to ensure the stable welding quality. In case the stabilized tool temperature cannot achieve higher than the critical temperature at the desired feed rate and maximum spindle rotation speed, then other approaches such as modification of the tool geometry to increase the frictional heat generation can be considered.

3.4.2. Welding length for tool temperature stabilization

In the early stage of the FSW process, the tool temperature was not stabilized. It infers that the welding quality is not stable especially under the critical tool temperature before the tool temperature stabilization. In terms of FSW process control, this means that time and welding length for tool temperature stabilization should be sufficiently set and the welding region with not stabilized tool temperature should avoid structural important features or positions of workpieces. Fig. 8b presents the required temperature stabilization length (l_{stbl}) shown in Fig. 8a. The stabilization length was defined as the required welding length to achieve at least 86.5% of stabilization temperature, only in terms of tool temperature regardless of welding quality. Therefore, it can be calculated simply by the feed rate as an FSW process parameter and the characteristic time, t_2 as an extracted tool temperature profile feature.

The slope was decreased according to the feed rate because of the decreasing t_2 in accordance with the feed rate (c.f., Fig. 6f). However, the stabilization length showed an overall linear relationship to the feed rate. This is because the converging relationship of t_2 to the feed rate as shown in Fig. 6f. t_2 can be regarded as constant, approximately 10 s in the high feed rate above 500 mm/min. Therefore, the required welding length for tool temperature stabilization can be determined proportionally to the feed rate range >500 mm/min.

4. Discussion

The developed real-time wireless FSW tool temperature measurement system would be effective for the practical monitoring of the FSW process. It can be compatible with conventional tool holders with minimized modifications for the measurement base. Furthermore, widely used IoT devices were utilized as main components for data acquisition and wireless data transmission. Therefore, the overall cost was relatively lower than conventional FSW tool temperature monitoring solutions, and the influence of the supply chain crisis such as the pandemic would be minimized. Even with the low cost, the wireless FSW tool temperature measurement system could measure and transfer multiple temperature data from the FSW tool and plot temperature profiles in real-time. Therefore, it could be utilized not only for FSW process monitoring but also for process control and optimization based on the tool temperature.

Temperature profiles measured from the FSW tool included various information on the FSW process, and they were closely related to the welding quality of the FSWed joint. The stages of the FSW process such as probe contact, shoulder contact with the workpiece, and tool forward can be distinguished by the transient temperature profiles measured from the probe and shoulder positions. Therefore, FSW engineers on the shop floor do not need to observe the FSW process at the side of the FSW machine. The tool temperature profile data can be accumulated and managed to further trace welding quality or defects. For example, a temperature value at a specific time corresponding to a specific defect position can be traced to figure out the cause of the defects. This is because tool temperature significantly affects welding quality and the position along the welding line corresponds to the time of the tool temperature profile data.

Tool temperature profiles measured from the different positions and depths were similar to each other. The most sensitive and fast responsive position for FSW tool temperature measurement was the probe. Therefore, measuring only the probe temperature would be the most cost-effective option for tool temperature measurement. The proposed wireless temperature measurement system can be minimized in terms of cost and size, as well.

Tool temperature-based FSW process control would have an advantage over naïve process parameter-based control because tool temperature represents actual FSW conditions where the material softened and stirred. The combination of the FSW process parameters to achieve higher tool temperature than the critical tool temperature for stabilized and high UTS as welding quality. Therefore, it is recommendable that control of the FSW process parameters to achieve higher tool temperature than the critical tool temperature. Spindle rotation speed is appropriate for the main control parameter. The exponential relationship between the required minimum spindle rotation speed to achieve the critical tool temperature and the feed rate (c.f., Fig. 7f) can be used for the development of a model-based closed-loop control method for spindle rotation speed. The linear relationships between stabilized tool temperature and spindle rotation speed (c.f., Fig. 6c) can be used, as well.

The required welding length for tool temperature stabilization was proportional to the feed rate. However, it could not be extended sufficiently in the limited size or structural constraints of workpieces. Applying sufficient dwell time to heating the tool temperature prior to tool forward movement could be an option. The tool forward movement can be triggered by the real-time tool temperature measurement. The dwell stage stops when the tool temperature exceeds the critical tool temperature, and then the tool forward movement stage can be initiated. It can minimize the welding length for tool temperature stabilization.

The required time to achieve tool temperature stabilization or the critical tool temperature would be a factor increasing the FSW process cycle time and reducing productivity. A variable spindle rotation speed would reduce the required time. Applying higher spindle rotation speed for early FSW process stages such as dwell or initial tool forward stages can accelerate the temperature increase rate due to higher frictional heat generation. After achieving the critical tool temperature or the desired tool temperature, the spindle rotation speed could be reduced.

The transient tool temperature which is measured at the inside of the tool would have a lagging time response from the tool-workpiece interface temperature. For example, the temperature at the shoulder (Shoulder dist. 1 mm in Fig. 5c) had about 0.7 s of lagged time response to the probe for the onset of the temperature increase, as shown in Fig. 5c. The distance between the thermocouple junctions of the shoulder (distance 1 mm from the shoulder surface) and the probe was about 5 mm. The distance from the probe surface and the thermocouple junction at the probe was 2.5 mm. Therefore, the lagged time response might be 0.35 s which is half of the time difference between the onset of the temperatures at the probe and shoulder. The lagging time response is inevitable. This is because the thermocouples were flush-mounted inside of the tool for better reliability and the distance between the tool-workpiece interface and the thermocouples acts as a heat transfer path. Therefore, to develop a closed-loop control method based on the tool temperature measurement, this lagging time response should be calibrated as proposed in by Fehrenbacher et al. [41], and Schmale et al. [39].

Installation of bare junction-type thermocouples at the tool-workpiece interface would be the best for the fastest response of the measured tool temperature to the variation of the actual FSW condition. It has been reported that the eccentric thermocouple position in the probe and shoulder induces a high-frequency oscillating temperature profile with a 10–15 ˚C amplitude [41], and the amplitude of the oscillating temperature was smaller at the smaller eccentric position of the thermocouple [39], as well. Therefore, a bare junction-type thermocouple installed at the center of the probe and tool (probe)-workpiece interface would be the best for the immediate response without an oscillating profile. However, it could not be practically appropriate for long-term application. This is because the cement or adhesive for thermocouple installation, or the thermocouple alloy such as alumel and chromel would be the weak point of the FSW tool. Therefore, it is desired to develop a durable installation method for thermocouples or other types of temperature sensors such as thermistors at the tool-workpiece interface.

4.1. Limitations and further research

The range of the tested FSW process parameters, especially feed rate, is difficult to include practical high-speed FSW processes. For example, 1,000 mm/min of feed rate could be too slow to get good productivity for larger parts. In addition to the considered process parameters, several process parameters such as FSW tool lead or tilt angle, downward force, plunge depth, gap between the probe and backing plate were not considered as process variables for this study. Therefore, the developed wireless FSW tool temperature measurement system will be

applied to the FSW process of large components such as aerospace applications, and the relationship among further process parameters, tool temperature profiles, and welding quality will be investigated.

Even though the mainly investigated temperature profile was measured in the probe and it showed a similar trend to the other profiles, it is not the perfectly same. Therefore, the temperature profile features of each temperature profile are different from other profiles. However, it will be difficult to manually analyze the relationship among the several FSW process parameters, multiple tool temperature profiles, and various welding quality factors. Recently developed explainable artificial intelligence (XAI) is applied to extract underlying patterns and knowledge in data by proposing reasonable explanations for the prediction or decision results of artificial intelligence (AI) models. Therefore, XAI will be applied to autonomous analysis of the effect of multiple FSW tool temperature profiles on the welding quality, and the relationship between the FSW process parameters and tool temperature profiles. XAI results will be applied to set intelligent FSW process monitoring windows and process control based on the effect of tool temperature features on welding quality.

5. Conclusion

Tool temperature is important process data presenting the actual friction stir welding (FSW) condition where the frictional heat is generated, and workpiece material is softened and stirred. Measuring this FSW tool temperature requires wireless temperature measurement and the relationship among the FSW process parameters, FSW tool temperature, and welding quality should be analyzed to utilize the FSW tool temperature for process improvement, control, and optimization. In this study, a real-time wireless FSW tool temperature measurement system was developed, and tool temperature profiles were measured at various positions and depths in the FSW tool in diverse FSW process conditions. The effect of representative tool temperature profile on welding quality and the influence of the FSW process parameters on tool temperature profile were investigated. As a result, the FSW process window for stable welding quality, and process control strategy were proposed based on the FSW tool temperature.

The proposed real-time wireless FSW tool temperature measurement system is cost-effective and applicable to the practical FSW process. It provides detailed tool temperature profile data in situ of the FSW process. The stabilized tool temperature, as one of the tool temperature profile features, has a close relationship to the ultimate tensile strength (UTS) of FSWed joint as welding quality. Regardless of the process parameters, the UTS converged higher stabilized value at the above critical tool temperature. Therefore, achieving and maintaining tool temperature higher than the critical tool temperature is important to setup FSW process and stable welding quality.

The spindle rotation speed can be used as the main parameter for tool temperature control because it directly changes the tool temperature. In higher feed rate FSW conditions, the required minimum spindle rotation speed to achieve the critical tool temperature is increased exponentially. Therefore, the spindle rotation speed is as important for welding quality as the feed rate for higher productivity. A minimum welding length, which is proportional to the feed rate should be guaranteed to achieve tool temperature stabilization. The welding line region without tool temperature stabilization should be avoided from the structurally important welding positions due to low welding quality. Therefore, a longer stabilization length or dwell time should be applied for higher-speed (feed rate) FSW processes. This tool temperature-based FSW process analysis is enabled by the wireless FSW tool temperature measurement. Therefore, it is recommendable to measure the FSW tool temperature for better FSW process monitoring, control, and optimization.

The proposed wireless FSW tool temperature measurement and its application to process monitoring and control are expected to relieve the tacit knowledge aspects of the FSW process, and contribute to autonomous and data-based manufacturing in the FSW industry.

Declaration of competing interest

The authors declare that they have no known competing financial interest or personal relationships that could have appeared to influence the work reported in this paper.

Data availability

Research data are not shared.

Acknowledgement

This research has been conducted with the support of the Korea Institute of Industrial Technology (KITECH) research project entitled “Predicting the quality of friction stir weld joint on curved lines using XAI (KITECH JE240016).” This research was funded by the ‘New Faculty Research Support Grant’ at Changwon National University in 2024, as well. The authors thank KAMTIC (KITECH – Auburn University Manufacturing Technology Innovation Center) for administrative support for this international research cooperation.

References

[1] Chen T. Process parameters study on FSW joint of dissimilar metals for aluminum-steel. J Mater Sci 2009;44:2573–80. https://doi.org/10.1007/s10853-009-3336-8.

[2] Lorrain O, Favier V, Zahrouni H, Lawrjaniec D. Understanding the material flow path of friction stir welding process using unthreaded tools. J Mater Process Technol 2010;210:603–9. https://doi.org/10.1016/j.jmatprotec.2009.11.005.

[3] Morishige T, Kawaguchi A, Tsujikawa M, Hino M, Hirata T, Higashi K. Dissimilar welding of Al and Mg alloys by FSW. Mater Trans 2008;49:1129–31. https://doi.org/10.2320/matertrans.MC200768.

[4] Boz M, Kurt A. The influence of stirrer geometry on bonding and mechanical properties in friction stir welding process. Mater Des 2004;25:343–7. https://doi.org/10.1016/j.matdes.2003.11.005.

[5] Rajakumar S, Balasubramanian V. Establishing relationships between mechanical properties of aluminium alloys and optimised friction stir welding process parameters. Mater Des 2012;40:17–35. https://doi.org/10.1016/j.matdes.2012.02.054.

[6] Babu S, Elangovan K, Balasubramanian V, Balasubramanian M. Optimizing friction stir welding parameters to maximize tensile strength of AA2219 aluminum alloy joints. Metals and Materials International 2009;15:321–30. https://doi.org/10.1007/s12540-009-0321-3.

[7] Rajakumar S, Muralidharan C, Balasubramanian V. Predicting tensile strength, hardness and corrosion rate of friction stir welded AA6061-T6 aluminium alloy joints. Mater Des 2011;32:2878–90. https://doi.org/10.1016/j.matdes.2010.12.025.

[8] Wang G, Zhao Y, Hao Y. Friction stir welding of high-strength aerospace aluminum alloy and application in rocket tank manufacturing. J Mater Sci Technol 2018;34:73–91. https://doi.org/10.1016/j.jmst.2017.11.041.

[9] Mishra RS, Ma ZY. Friction stir welding and processing. Materials Science and Engineering R: Reports 2005;50. https://doi.org/10.1016/j.mser.2005.07.001.

[10] Buffa G, Campanile G, Fratini L, Prisco A. Friction stir welding of lap joints: Influence of process parameters on the metallurgical and mechanical properties. Materials Science and Engineering: A 2009;519:19–26. https://doi.org/10.1016/j.msea.2009.04.046.

[11] Wahid MA, Sharma N, Shandley R. Friction stir welding process effects on human health and mechanical properties. vol. 1. 2020.

[12] Majeed T, Wahid MA, Alam MN, Mehta Y, Siddiquee AN. Friction stir welding: A sustainable manufacturing process. Mater Today Proc, vol. 46, Elsevier Ltd; 2020, p. 6558–63. https://doi.org/10.1016/j.matpr.2021.04.025.

[13] Tanaka T, Morishige T, Hirata T. Comprehensive analysis of joint strength for dissimilar friction stir welds of mild steel to aluminum alloys. Scr Mater 2009;61:756–9.

https://doi.org/10.1016/j.scriptamat.2009.06.022.

[14] Li B, Shen Y, Hu W. The study on defects in aluminum 2219-T6 thick butt friction stir welds with the application of multiple non-destructive testing methods. Mater Des 2011;32:2073–84. https://doi.org/10.1016/j.matdes.2010.11.054.

[15] Tan CW, Jiang ZG, Li LQ, Chen YB, Chen XY. Microstructural evolution and mechanical properties of dissimilar Al-Cu joints produced by friction stir welding. Mater Des 2013;51:466–73. https://doi.org/10.1016/j.matdes.2013.04.056.

[16] Jaiganesh V. An detailed examination on the future prospects of friction stir welding-a green technology. 2014.

[17] Sahu PK, Pal S, Pal SK, Jain R. Influence of plate position, tool offset and tool rotational speed on mechanical properties and microstructures of dissimilar Al/Cu friction stir welding joints. J Mater Process Technol 2016;235:55–67. https://doi.org/10.1016/j.jmatprotec.2016.04.014.

[18] Unnikrishnan MA, Edwin Raja Dhas J, Anton Savio Lewise K, Varghese JC, Ganesh M. Challenges on friction stir welding of magnesium alloys in automotives. Mater Today Proc 2023. https://doi.org/10.1016/j.matpr.2023.03.789.

[19] Nagaraja S, Anand PB, Mariswamy M, Alkahtani MQ, Islam S, Khan MA, et al. Friction stir welding of dissimilar Al-Mg alloys for aerospace applications: Prospects and future potential. Reviews on Advanced Materials Science 2024;63. https://doi.org/10.1515/rams-2024-0033.

[20] Riahi M, Nazari H. Analysis of transient temperature and residual thermal stresses in friction stir welding of aluminum alloy 6061-T6 via numerical simulation. International Journal of Advanced Manufacturing Technology 2011;55:143–52. https://doi.org/10.1007/s00170-010-3038-z.

[21] Xue P, Xie GM, Xiao BL, Ma ZY, Geng L. Effect of heat input conditions on microstructure and mechanical properties of friction-stir-welded pure copper. Metall Mater Trans A Phys Metall Mater Sci 2010;41:2010–21. https://doi.org/10.1007/s11661-010-0254-y.

[22] Upadhyay P, Reynolds AP. Effects of thermal boundary conditions in friction stir welded AA7050-T7 sheets. Materials Science and Engineering: A 2010;527:1537–43. https://doi.org/10.1016/j.msea.2009.10.039.

[23] Park HS, Kimura T, Murakami T, Nagano Y, Nakata K, Ushio M. Microstructures and mechanical properties of friction stir welds of 60% Cu-40% Zn copper alloy. Materials Science and Engineering: A 2004;371:160–9. https://doi.org/10.1016/j.msea.2003.11.030.

[24] Su H, Wu CS, Bachmann M, Rethmeier M. Numerical modeling for the effect of pin profiles on thermal and material flow characteristics in friction stir welding. Mater Des 2015;77:114–25. https://doi.org/10.1016/j.matdes.2015.04.012.

[25] Shi L, Wu CS. Transient model of heat transfer and material flow at different stages of friction stir welding process. J Manuf Process 2017;25:323–39. https://doi.org/10.1016/j.jmapro.2016.11.008.

[26] Yang J, Wang D, Xiao BL, Ni DR, Ma ZY. Effects of rotation rates on microstructure, mechanical properties, and fracture behavior of friction stir-welded (FSW) AZ31 magnesium alloy. Metall Mater Trans A Phys Metall Mater Sci 2013;44:517–30. https://doi.org/10.1007/s11661-012-1373-4.

[27] Xue P, Ni DR, Wang D, Xiao BL, Ma ZY. Effect of friction stir welding parameters on the microstructure and mechanical properties of the dissimilar Al-Cu joints. Materials Science and Engineering: A 2011;528:4683–9. https://doi.org/10.1016/j.msea.2011.02.067.

[28] Kadian AK, Biswas P. The study of material flow behaviour in dissimilar material FSW of AA6061

and Cu-B370 alloys plates. J Manuf Process 2018;34:96–105. https://doi.org/10.1016/j.jmapro.2018.05.035.

[29] Zhang F, Su X, Chen Z, Nie Z. Effect of welding parameters on microstructure and mechanical properties of friction stir welded joints of a super high strength Al-Zn-Mg-Cu aluminum alloy. Mater Des 2015;67:483–91. https://doi.org/10.1016/j.matdes.2014.10.055.

[30] Liu FC, Ma ZY. Influence of tool dimension and welding parameters on microstructure and mechanical properties of friction-stir-welded 6061-T651 aluminum alloy. Metall Mater Trans A Phys Metall Mater Sci 2008;39:2378–88. https://doi.org/10.1007/s11661-008-9586-2.

[31] Zhang Z, Zhang HW. Numerical studies on controlling of process parameters in friction stir welding. J Mater Process Technol 2009;209:241–70. https://doi.org/10.1016/j.jmatprotec.2008.01.044.

[32] Khodaverdizadeh H, Mahmoudi A, Heidarzadeh A, Nazari E. Effect of friction stir welding (FSW) parameters on strain hardening behavior of pure copper joints. Mater Des 2012;35:330–4. https://doi.org/10.1016/j.matdes.2011.09.058.

[33] Fujii H, Cui L, Maeda M, Nogi K. Effect of tool shape on mechanical properties and microstructure of friction stir welded aluminum alloys. Materials Science and Engineering: A 2006;419:25–31. https://doi.org/10.1016/j.msea.2005.11.045.

[34] Fehrenbacher A, Duffie NA, Ferrier NJ, Pfefferkorn FE, Zinn MR. Toward automation of friction stir welding through temperature measurement and closed-loop control. J Manuf Sci Eng 2011;133. https://doi.org/10.1115/1.4005034.

[35] Fehrenbacher A, Duffie NA, Ferrier NJ, Pfefferkorn FE, Zinn MR. Effects of tool-workpiece interface temperature on weld quality and quality improvements through temperature control in friction stir welding. International Journal of Advanced Manufacturing Technology 2014;71:165–79. https://doi.org/10.1007/s00170-013-5364-4.

[36] Anandan B, Manikandan M. Machine learning approach for predicting the peak temperature of dissimilar AA7050-AA2014A friction stir welding butt joint using various regression models. Mater Lett 2022;325. https://doi.org/10.1016/j.matlet.2022.132879.

[37] Sarvaiya J, Singh D. Prediction of performance parameters in friction stir processing using ANN and multiple regression models. Mater Today Proc 2023. https://doi.org/10.1016/j.matpr.2023.04.422.

[38] de Backer J, Bolmsjo G. Thermoelectric method for temperature measurement in friction stir welding. Science and Technology of Welding and Joining 2013;18:558–65. https://doi.org/10.1179/1362171813Y.0000000135.

[39] Schmale J, Fehrenbacher A, Shrivastava A, Pfefferkorn FE. Calibration of dynamic tool-workpiece interface temperature measurement during friction stir welding. Measurement (Lond) 2016;88:331–42. https://doi.org/10.1016/j.measurement.2016.02.065.

[40] Silva ACF, De Backer J, Bolmsjö G. Temperature measurements during friction stir welding. International Journal of Advanced Manufacturing Technology 2017;88:2899–908. https://doi.org/10.1007/s00170-016-9007-4.

[41] Fehrenbacher A, Duffie NA, Ferrier NJ, Pfefferkorn FE, Zinn MR. Effects of tool–workpiece interface temperature on weld quality and quality improvements through temperature control in friction stir welding. The International Journal of Advanced Manufacturing Technology 2014;71:165–79. https://doi.org/10.1007/s00170-013-5364-4.